DYNAMIC CHAOS IN RADIOPHYSICS
AND ELECTRONICS

Correlation Analysis of Deterministic and Noisy Chaos

V. S. Anishchenko, T. E. Vadivasova, G. A. Okrokvertskhov, and G. I. Strelkova

Abstract—Correlation and spectral properties of various chaotic self-sustained oscillations are analyzed. It is demonstrated that a few classical models of stochastic processes can be used to describe chaos autocorrelation functions. The effect of noise on stochastic systems is investigated.

INTRODUCTION

The analysis of correlation functions plays a key role in the studies of both stochastic (truly random) processes and chaotic oscillations generated by deterministic dynamics of nonlinear systems. There are several reasons for the importance of the correlation properties. The decrease in the correlation functions down to zero over long time intervals (splitting of correlations) is a consequence of mixing. If the time interval between the states of a system is rather long, they become statistically independent [1–5]. The ergodicity of a system follows from mixing. In addition, the splitting of correlations evolving in chaotic dynamic systems is related to instability of chaotic trajectories and entropy induced by a system [1–7]. A one-to-one relationship between the autocorrelation function of a process and its power spectrum is expressed through the Wiener-Khintchine transform. Power spectrum is an important characteristic used in applications.

At present, spectral and correlation properties of irregular oscillations in dynamic systems are still insufficiently studied in spite of their basic importance. It is commonly accepted that the correlation function of a chaotic system exponentially decays with a decrement determined by the Kolmogorov entropy H_K [3]. The Pesin theorem yields an upper estimate of entropy H_K equal to a sum of the positive Lyapunov exponents [5, 7, 8]. However, the theoretical results are available only for certain classes of discrete mixing-measure mappings. They yield an exponential upper estimate for the time decay of correlations [9, 10]. Sometimes, the correlation decay rate is related to Lyapunov exponents [11]. In other cases, it depends on the remaining characteristics determined by the Frobenius–Perron operator [12–15]. Even elementary mappings exhibit deviations from the exponential behavior [12]. For flow systems, theoretical estimates of the correlation decay rate are absent [16]. There are virtually no studies on numerical analysis of the correlation properties of chaos in flow systems.

In experiments, we normally analyze the autocorrelation function (ACF) of a certain dynamic variable of a system:

$$\psi(t, t + \tau) = \langle x(t)x(t + \tau) \rangle - \langle x(t) \rangle \langle x(t + \tau) \rangle, \quad (1)$$

where the angular brackets denote averaging over the ensemble of realizations of process $x(t)$. Chaotic oscillations can be treated as a stationary and ergodic process, so that $\langle x(t) \rangle \equiv$ const and $\Psi(t, t + \tau) = \psi(\tau)$, and the ensemble averaging can be replaced by time averaging over a single typical realization. It is convenient to normalize the autocorrelation function by its maximum value at $\tau = 0$: $\Psi(\tau) = \psi(\tau)/\psi(0)$.

Consider a few examples. Figure 1 shows normalized ACF $\Psi(m)$ of dynamic variable $x(n)$ of a two-dimensional (2D) mapping represented as

$$x(n + 1) = x(n) + y(n), \quad \mod 1,$$
$$y(n + 1) = x(n) + 2y(n), \quad \mod 1, \quad (2)$$

where n is discrete time, $m = n - n_0$ is the difference between time moments, and mod 1 denotes retaining of the fractional part. Toral diffeomorphism (2) represents a classical example of the C Anosov systems [13]. Therefore, the theorem on the exponential estimate of the correlation decay must be valid for mapping (2). It is clearly seen from Fig. 1 that ACF $\Psi(m)$ decays more
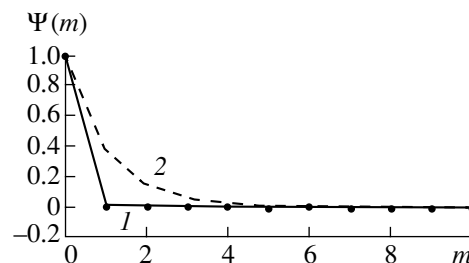
Fig. 1. (*1*) Normalized ACF of dynamic variable $x(n)$ of mapping (2) and (*2*) its exponential estimate $\exp(-|m|H_K)$.
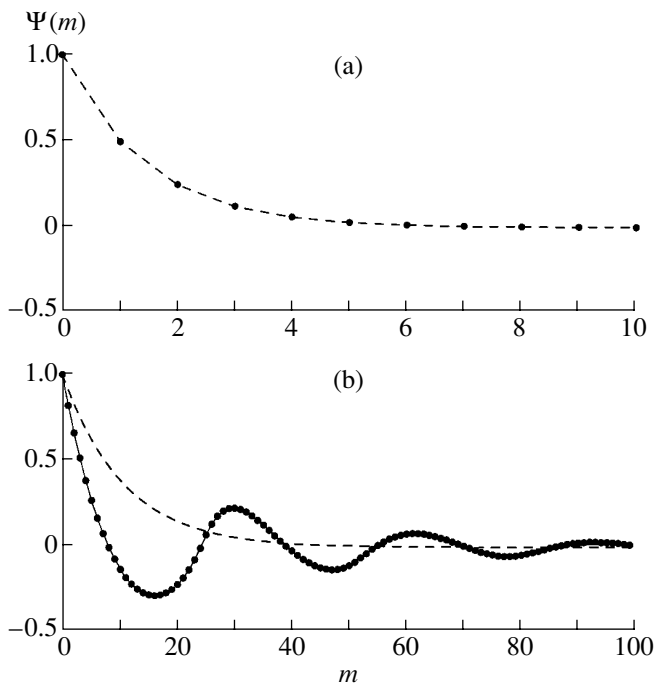
Fig. 2. Normalized ACF of a chaotic sequence $x(n)$ generated by mapping (3) at $K =$ (a) 2 and (b) 1.1: (dots) calculation and (dashed line) exponential estimate $\exp(-|m|\ln K)$. In case (a), the presence of a low-intensity noise makes it possible to avoid periodicity related to round-off errors at certain integer values of K.

Fig. 3. (Solid line) normalized ACF of chaotic sequence $x(n)$ generated by mapping (4) and (dashed line) its approximation based on expression (5) at (a) $\alpha = 2.83$ (in expression (5), $b = 0$) and (b) $\alpha = 2.84$ (in expression (5), $a = 3.5$ and $b = 6.5$).

rapidly than $\exp(-|m|H_{\mathrm{K}})$ (curve *2*), where Kolmogorov entropy H_{K} strictly equals positive Lyapunov exponent λ^+. However, the correlation decay is not described by an exponential function.

Another example is a one-dimensional (1D) stretching mapping given by

$$x(n + 1) = Kx(n), \quad \mathrm{mod}\,1. \qquad (3)$$

At $K > 1$, 1D noninvertible mapping (3) represents an elementary model chaotic system, for which the mixing property is proved [13, 18]. Using approximate analytical methods, it can be demonstrated that, for integer $K \gg 1$, the autocorrelation function of process $x(n)$ exponentially decays with a decrement equal to $\ln K$, which corresponds to the Kolmogorov entropy (the positive Lyapunov exponent) [3]. Numerical calculations show that the exponential law $\Psi(m) = \exp(-|m|\ln K)$ is valid even for integer $K \geq 2$ (Fig. 2a). For noninteger K and, especially, for the values of K close to unity, the ACF decay can substantially differ from the exponential function (Fig. 2b).

The autocorrelation function oscillations (see, for example, Fig. 2b) can be attributed to a certain periodicity of the chaotic process. A partial periodicity yields a periodic prefactor at the exponential.

Finally, consider the mapping that demonstrates chaotic intermittency in a certain range of parameter values:

$$x(n + 1) = (\alpha x(n) - x^3(n))\exp\!\left(-\frac{x^2(n)}{10}\right). \qquad (4)$$

At $\alpha = 2.83$, the system exhibits two chaotic attractors that are symmetric with respect to the point $x = 0$. The ACF curve, characterizing the correlation decay rate, is bounded from above by the exponential function $\exp(-|m|\lambda^+)$ (Fig. 3a). If $\alpha = 2.84$, we observe chaotic switching between the merged attractors (chaos–chaos intermittency [19]). Mean time T of stay at each of the merged attractors represents the second characteristic scale of mixing in addition to the first one related to λ^+. In this case (as well as in the case of the noise-induced switching [20]), the ACF can be approximated by the function

$$\Psi(m) = a\exp(-|m|\lambda^+) + b\exp(-2|m|/T), \qquad (5)$$

where a and b are constants. Figure 3b shows the corresponding results.

There are numerous reasons for the complexity of the ACF time dependence typical of the major part of chaotic systems. Note the heterogeneity of the properties of local instability in the phase space leading (as

was demonstrated in [3]) to a slow asymptotics of the ACF, the existence of nearly periodic oscillations, and the presence of the switching effects. All the features above are characteristic of nonhyperbolic chaotic attractors [21–23] representing the major part of chaotic attractors observed in the models of real dynamic systems. Also, for almost hyperbolic attractors (such as the Lorenz attractor [21, 24, 25]), the rate of splitting of correlations depends, to a great extent, not only on the rate of the exponential separation of trajectories.

In this work, we study the correlation and spectral properties of chaotic oscillations for the main types of chaotic attractors realized in autonomous differential systems with a three-dimensional (3D) phase space. The objects under study are classical models of nonlinear dynamics such as Rössler oscillator [26], Lorenz system [27], and a mathematical model of the Anishchenko–Astakhov oscillator, representing a radio device [19]. The purposes of this work are to determine the features of chaotic dynamics determining the rate of splitting of correlations and the width of the fundamental spectral line and to analyze the effect of noise on spectral and correlation characteristics of chaos. Based on the results of computer simulation, we demonstrate the correspondence (in terms of the correlation properties) between various types of chaotic oscillations and such basic models of stochastic processes as harmonic noise and a telegraph signal.

1. HARMONIC NOISE AND A TELEGRAPH SIGNAL

The analysis of applied problems often involves such models of random processes as noisy harmonic oscillations and a telegraph signal. The former is used to describe the effect of natural and technical fluctuations on the spectral and correlation characteristics of the output signal of quasi-harmonic self-sustained oscillators [29–31]. A telegraph random process is a model enabling one to describe statistical properties of pulse random processes, for example, random switching in a bistable system in the presence of noise (the Kramers problem, noise-induced switching of the Schmitt trigger, etc. [31–33]). The results of the studies of chaotic oscillations in 3D differential systems show that one can use the aforementioned classical models of random processes to describe spectral and correlation properties of a certain class of chaotic systems. Below, we demonstrate that the harmonic noise model describes the correlation characteristics of spiral chaos well and that the random telegraph signal model can be used to characterize the statistical properties of switching attractors, such as attractors in the Lorenz system [27] and Chua circuit [28].

Consider the main properties of the aforementioned classical models of random processes.

Harmonic Noise

Harmonic noise $x(t)$ represents a stationary random process with zero mean described by the oscillations given by [29–31]

$$x(t) = R_0[1 + \rho(t)]\cos[\omega_0 t + \phi(t)]. \qquad (6)$$

Here, R_0 and ω_0 are constant (mean) values of the oscillation amplitude and frequency and $\rho(t)$ and $\phi(t)$ are random functions characterizing amplitude and phase fluctuations, respectively. Assume that $\rho(t)$ is a stationary process. The harmonic noise model implies that the amplitude and phase fluctuations are slow compared to $\cos\omega_0 t$. The following simplifying assumptions are most frequently used: (i) amplitude and phase fluctuations are statistically independent and (ii) phase fluctuations represent a Wiener process written as

$$\dot{\phi}(t) = \sqrt{2B}\xi(t), \qquad (7)$$

where $\xi(t)$ is the normalized Gaussian white noise ($\langle\xi(t)\rangle \equiv 0$ and $\langle\xi(t+\tau)\xi(t)\rangle = \delta(\tau)$). Constant B is the phase diffusion coefficient. Under these assumptions, the ACF of process (6) is represented as [29–31]

$$\psi(\tau) = \frac{R_0^2}{2}[1 + K_\rho(\tau)]\exp(-B|\tau|)\cos\omega_0\tau, \qquad (8)$$

where $K_\rho(\tau)$ is the covariance function of reduced amplitude fluctuations $\rho(t)$.[1] Power spectral density can be obtained from expression (8) using the Wiener–Khintchine transform.

The Generalized Telegraph Signal

This stochastic process represents random switching between two possible states $x(t) = \pm a$. There are two main types of the telegraph process. The first one (a so-called random telegraph signal) is characterized by the Poisson distribution of switching moments t_k. In the stationary case, the mean frequency of switching is constant. The Poisson distribution of t_k results in the exponential distribution of pulse duration θ:

$$p(\theta) = n_1\exp(-n_1\theta), \quad \theta \geq 0, \qquad (9)$$

where n_1 is the mean switching frequency. The ACF of such a process is written as [31, 34]

$$\psi(\tau) = a^2\exp(-2n_1|\tau|). \qquad (10)$$

The other type of telegraph process (a quasi-random telegraph signal) corresponds to random switching between two states $x(t) = \pm a$ that can take place only at discrete moments $t_n = nT_0 + \eta$, $n = 1, 2, 3, \ldots$, where

---

[1] The prefactor $\dfrac{R_0^2}{2}[1 + K_\rho(\tau)]$ is covariance function $K_A(\tau)$ of random amplitude $A(t) = R_0[1 + \rho(t)]$. (It is convenient to use such a representation below.)

T_0 = const and η is a random quantity uniformly distributed over the interval $[0, T]$. Let p and q be the probabilities of the absence and presence of switching at a current moment, respectively. Then, the ACF of such a process is given by

$$\psi(\tau) = a^2(n - |\tau|/T_0)(p - q)^{n-1}$$
$$+ a^2[|\tau|/T_0 - (n - 1)](p - q)^n, \quad (11)$$
$$(n - 1)T_0 \le \tau < nT_0.$$

In the special case when the probabilities are $p = q = 1/2$, the ACF exhibits a linear decrease with time (Fig. 4):

$$\psi(\tau) = a^2(1 - |\tau|/T_0) \quad \text{at} \quad |\tau| < T_0;$$
$$\psi(\tau) = 0 \quad \text{at} \quad |\tau| < T_0, \quad (12)$$

2. CORRELATION AND SPECTRAL ANALYSIS OF SPIRAL CHAOS

Spiral (or phase-coherent) attractors emerge in the vicinity of the saddle–focus separatrix loop owing to period-doubling bifurcations. They are classified as chaotic attractors of the nonhyperbolic type [19, 35]. The power spectrum of spiral chaos exhibits a pronounced peak at the center (mean) frequency. As a consequence, the ACF envelope decays rather slowly, which can be illustrated by such examples as spiral attractors in the Rössler model [26], the Anishchenko–Astakhov oscillator with inertial nonlinearity [19], Chua circuit [28], etc. The corresponding self-sustained oscillations resemble the dynamics of noisy periodic oscillators (e.g., the Van der Pol oscillator). In particular, they exhibit a finite-width spectral line peaked at the basic frequency [36] and the effects of forced and mutual synchronization [37, 38]. From the physical point of view, such chaotic attractors have the properties of a noisy limit cycle. However, the spiral attractors are realized in deterministic systems (in the absence of noise).

Consider spiral chaos in the Rössler system represented as

$$\dot{x} = -y - z + \sqrt{2D}\xi(t), \quad \dot{y} = x + \alpha y,$$
$$\dot{z} = \beta - z(\mu + x), \quad \alpha = \beta = 0.2, \quad \mu = 6.5, \quad (13)$$

where $\xi(t)$ is the normalized Gaussian source of the δ-correlated noise with zero mean and D is the noise intensity. To introduce instantaneous amplitude $A(t)$ and total instantaneous phase $\Phi(t)$ of chaotic oscillations corresponding to the spiral attractor of the Rössler system, one can use the change of variables[2]

$$x(t) = A(t)\cos\Phi(t), \quad y(t) = A(t)\sin\Phi(t). \quad (14)$$

---

[2] This is possible owing to a virtually regular rotation of the *XY* trajectory projection around the saddle–focus. Note that the saddle–focus is close to the origin, so that one can neglect the constant components of oscillations $x(t)$ and $y(t)$.
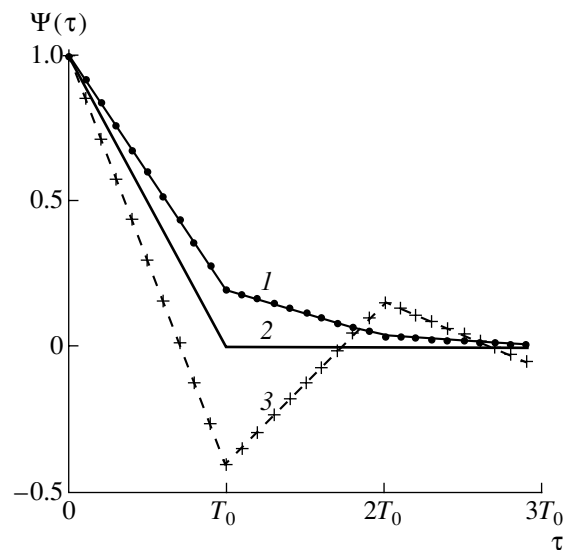
Fig. 4. ACFs of a quasi-random telegraph signal at the probabilities $p =$ (*1*) 0.6, (*2*) 0.5, and (*3*) 0.3.

With this change of variables, we can derive from expressions (13) the following system of equations:

$$\dot{A} = \frac{1}{2}\alpha A - \frac{1}{2}\alpha A \cos 2\Phi - z\cos\Phi + \sqrt{2D}\xi\cos\Phi,$$

$$\dot{\Phi} = 1 + \frac{1}{2}\alpha\sin 2\Phi + \frac{1}{A}z\sin\Phi - \frac{\sqrt{2D}}{A}\xi(t)\sin\Phi, \quad (15)$$

$$\dot{z} = \beta + z(A\cos\Phi - \mu).$$

In the calculations, both equivalent systems (13) and (15) are used.

Farmer [36] assumes that there exists a relationship between the width of the fundamental spectral line and ACF decay rate in the case of spiral chaos with phase fluctuations. However, the author does not introduce phase characteristics and performs no calculations supporting the assumption. Simulations [39] show that the Rössler system with developed spiral chaos exhibits a virtually linear increase in the variance of the instantaneous phase with time both in the absence of noise ($D = 0$) and at $D \ne 0$. The variance of the total phase equals the variance of its irregular component: $\phi(t) = \Phi(t) - \omega_0 t$, where $\omega_0 = \langle\dot{\Phi}(t)\rangle$ is the mean frequency of chaotic oscillations. The linear growth of variance $\sigma_\phi^2(t)$ makes it possible to introduce the effective phase diffusion coefficient:

$$B_{\text{eff}} = \frac{1}{2}\frac{d\sigma_\phi^2(t)}{dt}. \quad (16)$$

In simulations, we calculate the normalized ACF of chaotic oscillations $\Psi(\tau)$ in system (13). Using system (15), covariance function $K_A(\tau)$ of the amplitude
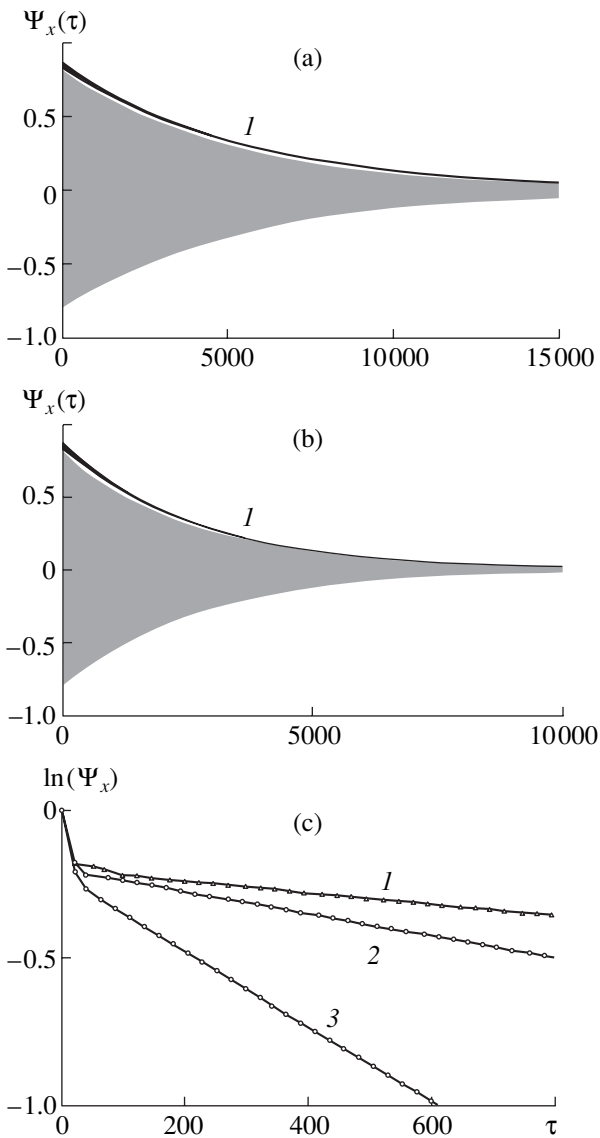
Fig. 5. (Gray area) normalized ACF of oscillations $x(t)$ in system (13) at $\alpha = \beta = 0.2$ and $\mu = 6.5$ and (*1*) its approximation based on expression (17) (a) in the absence of noise ($D = 0$) at $B_{\text{eff}} \approx 0.0002$ and (b) in the presence of noise at $D = 10^{-3}$ and $B_{\text{eff}} \approx 0.0003$. (c) ACF envelopes at logarithmic scale for $D = $ (*1*) 0, (*2*) 10^{-3}, and (*3*) 10^{-2}.

and effective phase diffusion coefficient B_{eff} are determined. The calculations of $\Psi(\tau)$ and $K_A(\tau)$ involve time averaging, whereas, in the calculations of B_{eff}, we perform averaging over the ensemble of realizations [39]. Figure 5 shows calculated ACF $\Psi(\tau)$ (gray dots). In both the absence and presence of noise (Figs. 5a and 5b, respectively), the ACF of chaotic oscillations decays virtually exponentially. At early moments ($\tau < 20$), the correlation decreases more rapidly (Fig. 5c) during a certain interval.

Proceeding from expression (8), we approximate the envelope of experimentally measured ACF $\Psi(\tau)$. To

this end, we substitute numerically calculated characteristics B_{eff} (16) and $K_A(\tau)$ into the expression for normalized envelope $\Gamma(\tau)$:

$$\Gamma(\tau) = \frac{K_A(\tau)}{K_A(0)} \exp(-B_{\text{eff}}|\tau|). \qquad (17)$$

Figures 5a and 5b demonstrate the results of calculation (gray area). It is seen that expression (17) describes the envelope of ACF $\Psi(\tau)$ well. Note that taking into account the ratio $K_A(\tau)/K_A(0)$ makes it possible to obtain a good approximation at both late ($\tau \geq 20$) and early ($0 < \tau < 20$) moments. This means that the amplitude fluctuations play a significant role at early moments, whereas slow splitting of correlations mainly depends on the effective phase diffusion. The coincidence of the experimental results for spiral chaos and the results obtained using the classical harmonic noise model is really amazing! However, we are unable to strictly account for such a coincidence. First of all, relationship (8) is obtained assuming that the values of amplitude and phase are statistically independent, which is not the case for chaotic oscillations. Second of all, expression (8) is derived assuming that phase fluctuations represent a Wiener process. In the case of chaotic oscillations, process $\phi(t)$ is more intricate and its statistical properties are unknown. Note that the data presented in Fig. 5a are obtained for deterministic chaos (in the absence of noise).

For $\tau > \tau_{\text{corr}}$ (where τ_{corr} is the correlation time), the chaotic oscillation ACF envelope is given by the exponential function $\exp(-B_{\text{eff}}|\tau|)$. In accordance with the Wiener–Khintchine theorem, the spectral peak at mean frequency ω_0 is close to Lorentzian, and its width depends on the effective phase diffusion coefficient B_{eff}:

$$S(\omega) = C \frac{B_{\text{eff}}}{B_{\text{eff}}^2 + (\omega - \omega_0)^2}, \quad C = \text{const.} \qquad (18)$$

This is proved by calculations (Fig. 6). The approximation of the central peak based on expression (18) agrees well with the direct simulations of the power spectrum of oscillations $x(t)$ in both the absence and presence of noise. Note that the results for the noise intensity $D = 10^{-3}$ (Figs. 5 and 6) were also verified for the noise intensities $0 < D < 10^{-2}$ and for other values of parameter μ corresponding to the spiral attractor mode.

The results of approximation of the chaotic oscillation ACF and the shape of the fundamental spectral peak agree with the studies of spiral attractors in alternative dynamic systems. For example, consider the Anishchenko–Astakhov oscillator with inertial nonlinearity [19]. With dimensionless variables, it is described by the following equations:

$$\dot{x} = mx + y - xz + rx^3 + \sqrt{2D}\xi(t),$$
$$\dot{y} = -x, \quad \dot{z} = -gz + gf(x), \qquad (19)$$
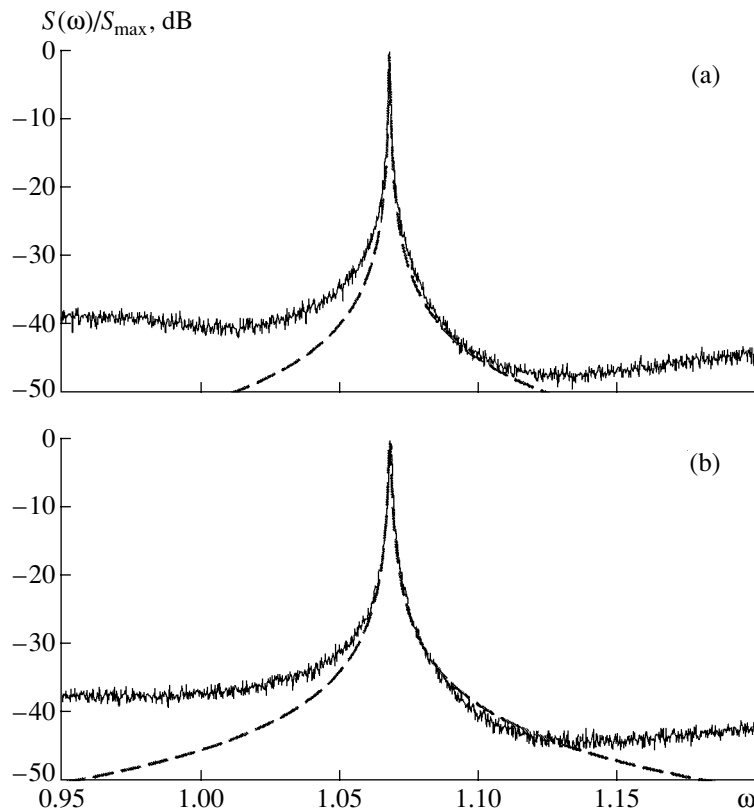
Fig. 6. (Solid line) fragment of the normalized power spectrum of oscillations $x(t)$ in system (13) in the vicinity of the center frequency at $\alpha = \beta = 0.2$ and $\mu = 6.5$ and (dashed line) its approximation based on expression (18) for $D = $ (a) 0 and (b) 10^{-3}.

where $f(x) = x^2$ at $x > 0$, $f(x) = 0$ at $x \leq 0$, $m = 1.35$, $g = 0.21$, and $\xi(t)$ is a noise source with the same characteristics as in system (13). We analyze equations (19) and equations obtained using change of variables (14). The oscillator with inertial nonlinearity is extremely sensitive to low-intensity noise. Compare systems (13) and (19). In the latter, a significantly lower noise leads to a substantially greater increase in the phase diffusion. In addition, the noise effect on a developed spiral attractor results in considerable qualitative changes and gives rise to funnel chaos. Figure 7 demonstrates a fragment of the power spectrum in the vicinity of the fundamental frequency and the approximation of the central peak based on (18). The calculations for system (19) are performed at two values of noise intensity.

Thus, the simulations clearly show that the spiral chaos in self-sustained oscillatory systems retains to a great extent the spectral and correlation properties of noisy quasi-harmonic self-sustained oscillations. At early moments, the rate of splitting of correlations in a flow system depends on both the instantaneous amplitude and the instantaneous phase of the chaotic oscillations. At late moments, the ACF envelope is mainly determined by the instantaneous phase diffusion. Correspondingly, the width of the main peak in the power spectrum of spiral chaos also depends on B_{eff}, and the instantaneous amplitude oscillations determine the

level of spectral pedestal. In the absence of noise, the effective phase diffusion coefficient depends on the chaotic dynamics of the system. However, there is no
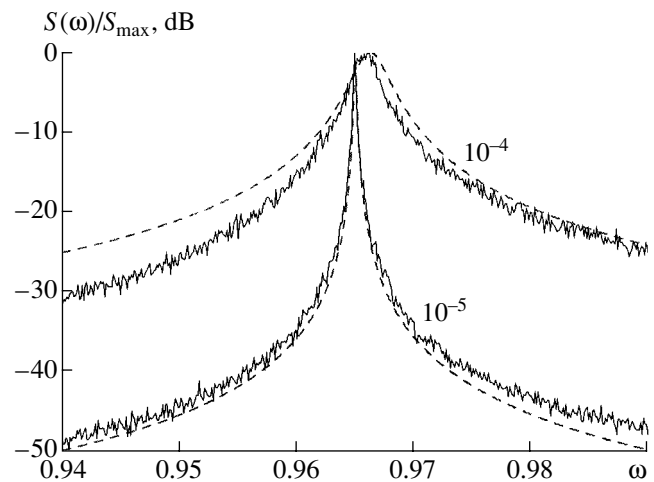
Fig. 7. (Solid lines) fragments of the normalized power spectrum of oscillations $x(t)$ in system (19) in the vicinity of the basic frequency at $\alpha = \beta = 0.2$ and $\mu = 6.5$ and (dashed line) its approximation based on expression (18) for two noise intensities $D = 10^{-4}$ ($B_{\text{eff}} \approx 0.0017$) and $D = 10^{-5}$ ($B_{\text{eff}} \approx 0.00008$).
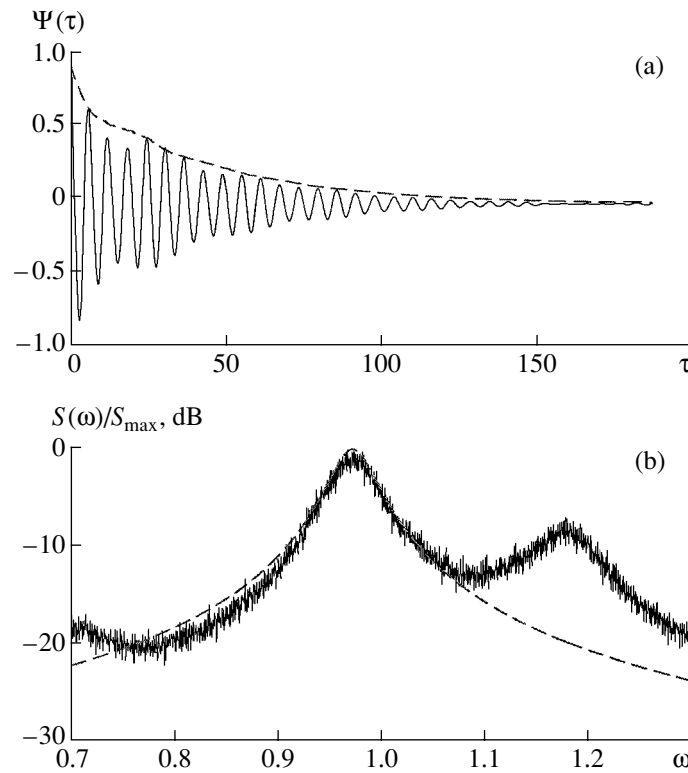
Fig. 8. (a) Normalized ACF and (b) (solid line) fragment of the normalized power spectrum of oscillations $x(t)$ in system (13) in the case of funnel chaos at $\alpha = \beta = 0.2$, $\mu = 13$, and $D = 0$. Dashed lines show approximations based on expressions (17) and (18). Diffusion coefficient is estimated to be $B_{\text{eff}} \approx 0.0219$.

direct relationship between this coefficient and the positive Lyapunov exponents. The Lyapunov exponents determine the properties of mixing only in the transverse cross section of the flow (i.e., in the Poincaré mapping).

3. ACFs AND POWER SPECTRA FOR FUNNEL CHAOS

The results obtained can be generalized, to a certain extent, to the funnel chaos mode. In comparison to spiral chaos, the funnel chaos attractor exhibits a more intricate rotation of the trajectory around the equilibrium point, which depends on the deterministic evolution operator. This rotation is accompanied by the jumps in the instantaneous phase leading to nonmonotonic time dependence of the phase (angular variable) [35, 39]. Funnel chaos is realized in system (13), studied in this work, at $\alpha = \beta = 0.2$ and $\mu > 8.5$.

To more strictly determine the instantaneous phase of oscillation $x(t)$ in a system with complex phase dynamics, one can use the concept of analytical signal [40, 41]. Analytical signal $\omega(t)$ is a complex function of time represented as

$$\omega(t) = x(t) + i\tilde{x}(t) = a(t)\exp(i\Phi(t)), \qquad (20)$$

where $x(t)$ is a stationary centered (with zero mean)

process and $\tilde{x}(t)$ is the Hilbert transform of original process $x(t)$:

$$\tilde{x}(t) = \frac{1}{\pi}\int\limits_{-\infty}^{\infty}\frac{x(t)}{t-\tau}d\tau. \qquad (21)$$

In this expression, the integral is considered in the sense of the Cauchy principal value. The convergence of the integral for stochastic process $x(t)$ is defined in the rms sense. Instantaneous phase (angular variable) $\Phi(t)$ of process $x(t)$ is given by

$$\Phi(t) = \arctan(\tilde{x}/x) + \pi k, \quad k = 0, 1, 2, 3, \ldots. \quad (22)$$

The value of k is determined taking into account the continuity of function $\Phi(t)$.

The transition to the funnel attractor results in a significant (by two to three orders of magnitude) increase in diffusion coefficient B_{eff} of deterministic chaos leading to a rapid decay of the ACF and a significant broadening of the main spectral peak [39].

Simulations for system (13) at $\mu = 13$ and $D = 0$ show that, for funnel chaos, the approximations under consideration can also provide adequate results (Fig. 8).

However, at certain values of parameter μ, the behavior of phase variable $\Phi(t)$ is so complicated that expression (17) fails to provide an adequate approxima-
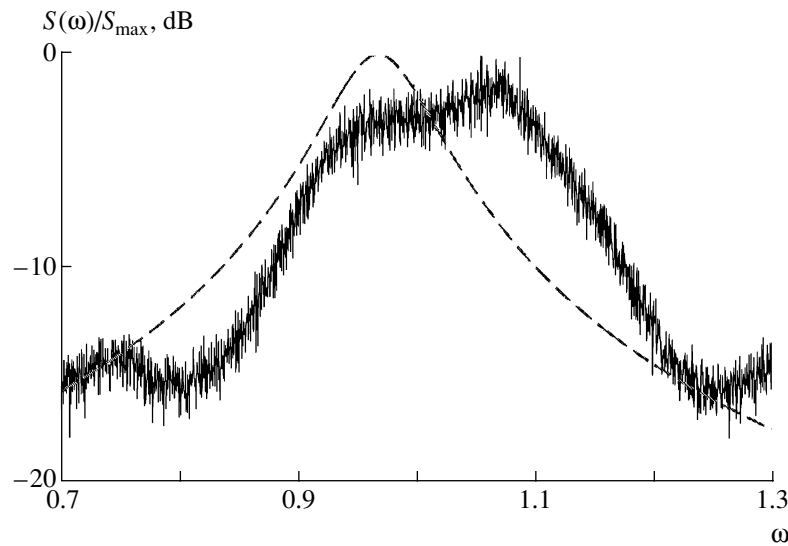
Fig. 9. (Solid line) fragment of the normalized power spectrum of oscillations $x(t)$ in system (13) in the case of funnel chaos at $\alpha = \beta = 0.2$, $\mu = 10$, and $D = 0$ and (dashed line) approximation based on expressions (18). Diffusion coefficient is estimated to be $B_{eff} = 0.0401$.
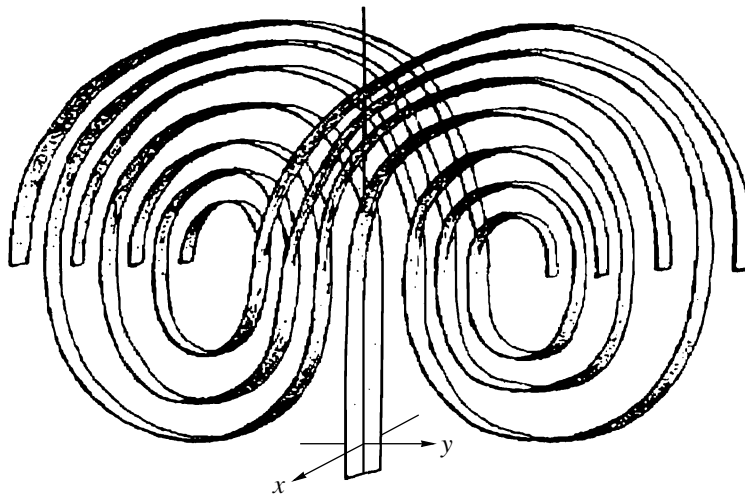
Fig. 10. Global structure of manifolds in the Lorenz system.

tion, and the main spectral peak is far from Lorentzian. This happens if the phase trajectories get into an infinitesimal neighborhood of the saddle–focus. We observe such a behavior at $\mu = 10$ (Fig. 9).

4. CORRELATION PROPERTIES OF THE LORENZ ATTRACTOR

The method above of analyzing the correlation properties of the Rössler and Anishchenko–Astakhov chaotic systems, which involves the effective phase diffusion coefficient, is inapplicable for the approximation of the ACFs of switching chaotic oscillations, when the phase space contains a few well-distinguished states visited by trajectories with a certain probability. In the trivial case, these states may represent stable points and cycles. However, in such systems, switching is possible only under the effect of noise or an external force [20, 32]. For a few rather complex chaotic attractors, one can also select the states representing parts of an attractor separated in a complicated way by a manifold of saddle points and cycles. The transitions between these states are possible at the moments defined by certain conditions [42]. Such oscillations arise, for example, in mapping (3) and in the Lorenz system given by

$$\dot{x} = -\sigma(x - y), \quad \dot{y} = -xz - y + rx, \quad \dot{z} = -bz + xy,$$
$$\sigma = 10, \quad b = 8/3, \quad r = 28. \tag{23}$$

In the phase space of the Lorenz system, there exist two saddle–focus points symmetric relative to the OZ
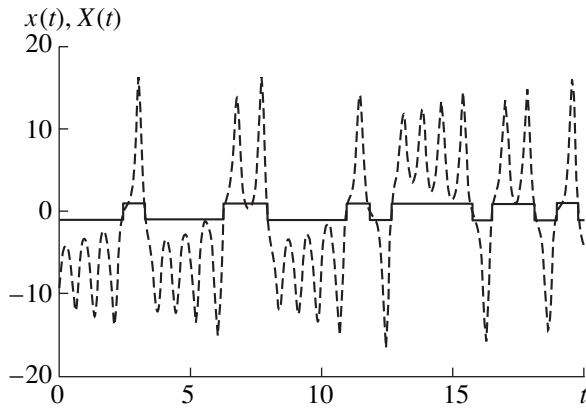
Fig. 11. Telegraph signal obtained for coordinate $x(t)$ of the Lorenz system.
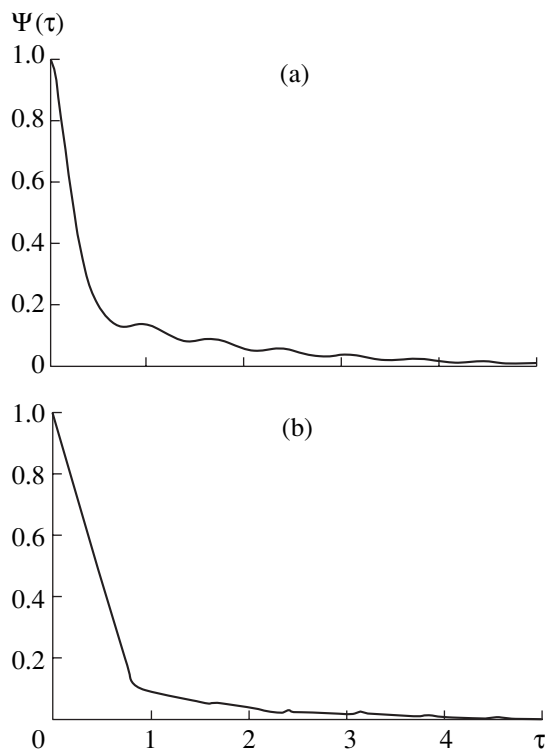
Fig. 12. ACFs of (a) realization $x(t)$ and (b) telegraph signal.

axis and separated by a stable saddle-point manifold at the origin. The complex structure of this stable manifold allows the transition of trajectories from one saddle–focus to another along certain paths (Fig. 10) [21, 42]. A trajectory untwisting around a saddle–focus comes to the stable manifold, from which it may jump with a certain probability to the other saddle–focus. It is most likely that the rotation around the saddle–focus points slightly affects the decay of the ACF. The ACF decay rate must be determined by random switching.

Consider the realization of the X coordinate of the Lorenz system (Fig. 11). Using the methods of sym-

bolic dynamics (i.e., eliminating oscillations (rotation around saddle–focus points)), one can obtain a switching process similar to the telegraph signal. Each of the two states of the system corresponds to the trajectory location in the vicinity of one of the saddle–focus points. The moment of switching between these states corresponds to the moment at which the trajectory crosses the YZ plane. In the presence of noise, the moment of switching corresponds to the moment of crossing a layer whose width depends on the noise intensity. To account for this, note that, immediately after crossing the boundary between the two states, the trajectory can be switched back by the noise, which corresponds to an infinitesimal switching time.

Compare the ACF of oscillation $x(t)$ in the Lorenz system and the ACF of given realization $x(t)$ of the telegraph signal (Fig. 12).

It can be concluded that the time of splitting of correlations and the ACF behavior at this time scale mainly depend on switching, whereas the rotation around the saddle–focus points slightly affects the ACF decay. Note the linear ACF decay at early moments. This is a remarkable fact in the sense that the linear ACF decay corresponds to a special probability distribution of the times of stay in one of the states. In Section 1, we have defined two telegraph signals using the distributions of the times of stay in one of the states. The linear ACF corresponds to a discrete equidistant distribution of the times of stay representing delta peaks, so that the switching probability equals 1/2 [31, 34].

Figure 13 demonstrates the distribution of pulse durations for the telegraph signal corresponding to chaotic switching with the Lorenz attractor.

It is seen that the distribution of the times of stay is close to an equidistant discrete distribution, although the peaks have finite widths. The probability distribution of switchings at the times divisible by T_0 (T_0 is the minimum time of stay in one of the states) shows that the probability of transition is close to 1/2. In agreement with the theoretical results [34], the ACF decreases to a finite value rather than to zero due to a finite width of the peaks in the distribution and the fact that the probability of transition slightly differs from 1/2.

The discreteness of switching in the Lorenz system depends on the features of the manifolds of the system. Manifold splitting in halves in the vicinity of the point ($x = 0$, $y = 0$) determines the behavior of the system trajectories, so that the probability of switching between two states per revolution around a fixed point equals 1/2. Owing to these features of the trajectory, the ACF of coordinates x and y must be determined by expression (12).

In the presence of a low-intensity Gaussian white noise, the linear character of the ACF remains virtually unchanged. As before, model (12) describes the ACF of the telegraph signal corresponding to $x(t)$ well, since
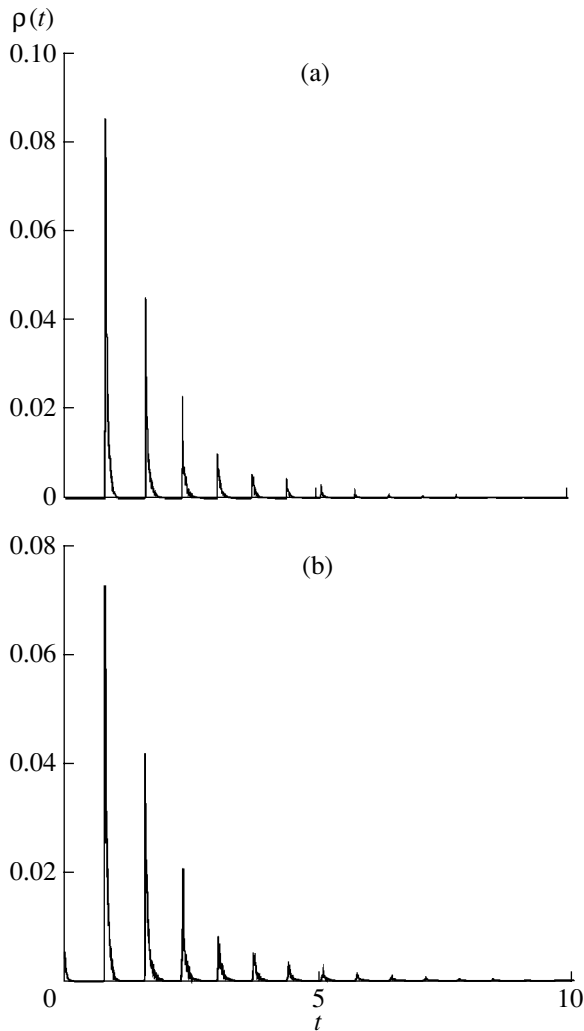
Fig. 13. The distribution of the pulse durations of the telegraph signal (a) in the absence of noise and (b) in the presence of noise at $D = 0.001$.

the character of the distribution of pulse durations remains the same (Fig. 13b).

CONCLUSIONS

The results of simulations show that spiral chaos substantially retains the properties of quasi-harmonic oscillations. At early moments, the rate of splitting of correlations in differential systems depends on both the behavior of the instantaneous amplitude and the diffusion of the instantaneous phase of chaotic oscillations. Therefore, the width of the fundamental spectral line of spiral chaos depends on the effective phase diffusion coefficient B_{eff}, whereas oscillations of the instantaneous amplitude determine the spectral pedestal level. In the absence of noise, coefficient B_{eff} depends not only on the positive Lyapunov exponents but also on the features of chaotic dynamics.

The studies of the Lorenz attractor show that the ACF properties depend on the statistics of chaotic switching of the phase trajectory between the neighborhoods of two saddle–focus points and slightly depend on the characteristics of rotation around these points. The correlation properties of chaotic oscillations are described well by the classical model of a quasi-random telegraph signal. In particular, expression (12) approximates the linear decrease in the ACF of oscillations $x(t)$ over the interval $\tau \in [0.2, 1]$ well.

REFERENCES

1. Billingsley, P., *Ergodic Theory and Information,* New York: Wiley, 1965.
2. Kornfel'd, I.P., Sinai, Ya.G., and Fomin, S.V., *Ergodicheskaya teoriya* (Ergodic Theory), Moscow: Nauka, 1980.
3. Zaslavskii, G.M., *Stokhastichnost' dinamicheskikh sistem* (Stochastic Behavior of Dynamic Systems), Moscow: Nauka, 1984.
4. Sinai, Ya.G., *Nelineinye volny* (Nonlinear Waves), Gaponov-Grekhov, A.V., Ed., Moscow: Nauka, 1979, p. 192.
5. Eckmann, J.P. and Ruelle, D., *Rev. Mod. Phys.,* 1985, vol. 57, no. 3, p. 617.
6. Kolmogorov, A.N., *Dokl. Akad. Nauk SSSR,* 1959, vol. 124, no. 4, p. 754.
7. Sinai, Ya.G., *Dokl. Akad. Nauk SSSR,* 1959, vol. 124, no. 4, p. 768.
8. Pesin, Ya.B., *Usp. Mat. Nauk*, 1977, vol. 32, no. 4, p. 55.
9. Bowen, R., *Equilibrium States and the Ergodic Theory of Anosov Diffeomorphisms. Lecture Notes in Mathematics*, Berlin: Springer, 1975.
10. Ruelle, D., *Am. J. Math.*, 1976, vol. 98, p. 619.
11. Ruelle, D., *Commun. Math. Phys.*, 1989, vol. 125, p. 239.
12. Christiansen, F., Paladin, G., and Rugh, H.H., *Phys. Rev. Lett.*, 1990, vol. 63, p. 2087.
13. Liverani, V., *Ann. Math.,* 1995, vol. 142, no. 2, p. 239.
14. Froyland, G., *Commun. Math. Phys.*, 1997, vol. 189, p. 237.
15. Ostruszka, A. and Zyczkowski, K., *Phys. Lett. A,* 2001 vol. 289, p. 306.
16. Bowen, R. and Ruelle, D., *Inventions Math.*, 1975, vol. 29, p. 181.
17. Arnol'd, V.I., *Dopolnitel'nye glavy teorii obyknovennykh differentsial'nykh uravnenii* (Additional Chapters

of the Theory of Ordinary Differential Equations), Moscow: Nauka, 1978.

18. Renyi, A., *Acta Math. Acad. Sci. Hungar.*, 1957, vol. 8, p. 477.

19. Anishchenko, V.S., *Slozhnye kolebaniya v prostykh sistemakh* (Complex Oscillation in Simple Systems), Moscow: Nauka, 1990.

20. Jung, P., *Phys. Rep.,* 1993, vol. 234, no. 175.

21. Shilnikov, L.P., *Int. J. Bifurcation Chaos*, 1997, vol. 7, no. 9, p. 1953.

22. Afraimovich, V.S., *Nonlinear Waves*, Gaponov, A.V., Rabinovich, M.I., and Engelbrechet, J., Eds., Berlin: Springer, 1989, p. 14.

23. Anishchenko, V.S., Astakhov, V.V., Neiman, A.B., *et al.*, *Nonlinear Dynamics of Chaotic and Stochastic Systems*, Berlin: Springer, 2002.

24. Afraimovich, V.S., Bykov, V.V., and Shil'nikov, L.P., *Dokl. Akad. Nauk SSSR*, 1977, vol. 234, p. 336.

25. Bykov, V.V. and Shil'nikov, L.P., *Metody kachestvennoi teorii i teorii bifurkatsii* (Methods of Qualitative Theory and Bifurcation Theory), Gor'kii: Izd. Gor'k. Univ., 1989, p. 151.

26. Rössler, O.E., *Phys. Lett. A*, 1976, vol. 57, p. 397.

27. Lorenz, E.N., *J. Atmos. Sci.*, 1963, vol. 20, p. 130.

28. *Chua'S Circuit: A Paradigm for Chaos*, Madan, R.N., Ed., Singapore: World Sci., 1993.

29. Stratonovich, R.L., *Izbrannye voprosy teorii fluktuatsii v radiotekhnike* (Selected Problems of Fluctuation Theory in Radio Engineering), Moscow: Sovetskoe Radio, 1961.

30. Malakhov, A.N., *Fluktuatsii v avtokolebatel'nykh sistemakh* (Fluctuations in Self-Oscillatory Systems), Moscow: Nauka, 1968.

31. Rytov, S.M., *Vvedenie v statisticheskuyu radiofiziku* (Introduction to Statistical Radio Physics), Moscow: Nauka, 1966.

32. Kramers, H.A., *Physica,* 1940, vol. 7, p. 284.

33. Hänggi, P., Talkner, P., and Borkovec, M., *Rev. Mod. Phys.*, 1990, vol. 62, p. 2.

34. Tikhonov, V.I. and Mironov, M.A., *Markovskie protsessy* (Markovian Processes), Moscow: Sovetskoe Radio, 1977.

35. Arneodo, A., Collet, P., and Tresser, C., *Commun. Math. Phys.*, 1981, vol. 79, p. 573.

36. Farmer, I.D., *Phys. Rev. Lett.,* 1981, vol. 47, no. 3, p. 179.

37. Anishchenko, V.S., Vadivasova, T.E., Postnov, D.E., and Safonova, M.A., *Int. J. Bifurcation Chaos*, 1992, vol. 2, no. 3, p. 633.

38. Rosenblum, M.G., Pikovsky, A.S., and Kurths, J., *Phys. Rev. Lett.*, 1996, vol. 76, no. 11, p. 1804.

39. Anishchenko, V.S., Vadivasova, T.E., Kopeikin, A.S., *et al.*, *Phys. Rev. E: Stat. Phys., Plasmas, Fluids, Relat. Interdiscip. Top.*, 2002, vol. 65, no. 2, p. 036206.

40. Vanshtein, L.A. and Vakman, D.E., *Razdelenie chastot v teorii kolebanii i voln* (Frequency Separation in Theory of Oscillations and Waves), Moscow: Nauka, 1983.

41. Bendat, J.S. and Piersol, A.G., *Random Data. Analysis and Measurement Procedures*, New York: Wiley, 1986. Translated under the title *Prikladnoi analiz sluchainykh dannykh,* Moscow: Mir, 1989.

42. Jackson, E.A., *Perspectives of Nonlinear Dynamics*, London: Cambridge University Press, 1989, vol. 1; 1991, vol. 2.